Off-grid radar detection strategy for the Normalized Matched Filter: achieving the GLRT performance

S. Trottier*†, J. Bosse*, O. Rabaste*, P. Forster‡, J.-.P Ovarlez*†
*DEMR, ONERA, Université Paris-Saclay, F-91120 Palaiseau, France.
†SONDRA CentraleSupélec, Université Paris-Saclay, F-91192 Gif-sur-Yvette, France.
‡Université Paris-Saclay, ENS Paris-Saclay, CNRS, SATIE, F-91190, Gif-sur-Yvette, France.

***Abstract*—A general problem in radar is to detect whether the received signal contains a specific signal of interest or not. We focus on one of the most widespread detectors: the Normalized Matched Filter. To be more realistic, we consider the case where the target can be off-grid. Currently, different methods exist to perform the off-grid Normalized Matched Filter test, but their detection performances are degraded if the noise is not white. In this paper, a new method based on reparametrization is proposed. While having a computational cost similar to state-of-the-art techniques, its detection performances are always better.**

***Index Terms*—Radar, Detection, Off-grid, Normalized Matched Filter, Reparametrization**

I. Introduction

A general problem in signal processing, appearing in many applications, such as radar, telecommunications, and seismology, is to detect whether a signal contains a specific signal of interest, hypothesis ($\mathcal{H}_1$) or not, hypothesis ($\mathcal{H}_0$). Detection theory provides different ways to solve such problems, but the likelihood ratio test (LRT) is the most common [1]. Performing the LRT requires the knowledge of all the scene parameters, which is often not possible. Hence, the Generalized LRT (GLRT) was proposed to overcome this issue, the principle of which is to replace the scene's unknown parameters with their maximum likelihood estimates [2].

We mainly focus on the monotarget Normalized Matched Filter (NMF) [3], also called adaptive cosine estimator [4], a very popular detector in the radar literature. In general, we do not know the parameters of the target and the objective is to compute the maximum of the NMF over the entire parameter space: the off-grid GLRT. Hence, the standard solution in the literature is to perform the NMF on a grid of parameters with possibly a monopulse estimate for refinement [5] in order to find the target position and to finally consider the maximum of all these tests. This implementation is very widespread both for simplicity reason and the fact that in radar, computational power and time are constrained.

To the best of our knowledge, the grid samples are regularly spaced because the false alarm rate of the on-grid NMF is constant on the grid points, so there was no particular reason to do otherwise. Moreover, in the white noise case, such vectors are orthogonal and define a partition of the space on an orthonormal basis, so without any additional information, taking a regular grid in the non-white noise case seems reasonable.

In practice, the targets are not on the grid, and the NMF is not efficient in detecting off-grid targets [6]. Hence, the grid points should be carefully chosen otherwise the NMF may fail. Moreover, it has recently been shown that the false alarm rate of the NMF, considering continuous intervals instead of points, is not uniform on the whole parameter space when the noise is not white anymore [7]. These two points suggest that more attention should be paid to the choice of the grid and that a regular grid may not be optimal.

A solution based on a regular grid has been proposed in [8] and allows one to ensure that the target is detected when the Signal-to-Noise Ration (SNR) is high enough. However, it still suffers from some drawbacks at lower SNR. In this paper, we propose a strategy to compute the off-grid NMF taking into account the impact of non-white noise. It is based on a reparametrization which induced a uniform distribution of the probability of false alarm. We show that such a choice is relevant as it also allows to take into account the main lobe deformation when the noise is not white. We show that our method yields the best known approximation of the true off-grid GLRT with a very low computational cost.

The paper is organized as follows. Section II formulates the problem. In Section III, we propose a new method for defining a grid of test points as a function of the noise covariance matrix. Section IV proposes a new way to perform the NMF-GLRT. Finally, Section V includes numerical experiments to highlight the benefits of this new method.

Notations: Italic type indicates a scalar quantity, lower case boldface indicates a vector quantity, and upper case boldface indicates a matrix or tensor. The transpose and transpose conjugate operators are ^{T} and ^{H} respectively. $\mathbf{x} \sim \mathcal{CN}(\boldsymbol{\mu}, \boldsymbol{\Sigma})$ is a random complex circular Gaussian vector with mean vector $\boldsymbol{\mu}$ and covariance matrix $\boldsymbol{\Sigma}$. The matrix trace operator is denoted as $\mathrm{Tr}(.)$. The derivative of a single parameter function f is denoted f' and the second-order derivative f''.

II. Problem formulation

In radar detection, the problem is to choose between two scenarios: the received signal, modeled as a complex N-vector $\mathbf{y}$, is either noise $\mathbf{n}$ or contains a signal of interest $\alpha\,\mathbf{a}(\theta)$ plus noise $\mathbf{n}$. Formally, it means deciding between two hypotheses:

$$\begin{cases} \mathcal{H}_0 : \mathbf{y} = \mathbf{n}\,, & \text{(noise)} \\ \mathcal{H}_1 : \mathbf{y} = \alpha\,\mathbf{a}(\theta) + \mathbf{n}\,, & \text{(signal + noise)} \end{cases} \tag{1}$$

where $\mathbf{n} \sim \mathcal{CN}\left(\mathbf{0}, \sigma^2\mathbf{R}\right)$. $\mathbf{R}$ is assumed to be known while its power σ^2 is not known [9], $\alpha \in \mathbb{C}$ is the target unknown amplitude, $\mathbf{a}(\theta)$ is a complex steering vector related to the target Doppler bin, defined as:

$$\mathbf{a}(\theta) = \frac{1}{\sqrt{N}}\left(1, e^{2i\pi\theta}, \ldots, e^{2i\pi(N-1)\theta}\right)^T, \tag{2}$$

with θ unknown and belonging to $\Theta = [0, 1[$.

The distribution of $\mathbf{y}$ under $\mathcal{H}_0$ depends only on $\boldsymbol{\lambda_0} = \{\sigma^2\}$ while the distribution of $\mathbf{y}$ under $\mathcal{H}_1$ depends on $\boldsymbol{\lambda_1} = \{\alpha, \sigma^2, \theta\}$.

The generalized likelihood ratio test (GLRT) consists in evaluating the ratio between two maximum likelihoods: the maximum likelihood of $\mathbf{y}$ assuming $\mathcal{H}_1(\boldsymbol{\lambda_1})$, over all possible values of $\boldsymbol{\lambda_1}$ and the maximum likelihood of $\mathbf{y}$ assuming $\mathcal{H}_0(\boldsymbol{\lambda_0})$, over all possible value of $\boldsymbol{\lambda_0}$:

$$\frac{\max\limits_{\boldsymbol{\lambda_1}} f_{\mathcal{H}_1}(\mathbf{y})}{\max\limits_{\boldsymbol{\lambda_0}} f_{\mathcal{H}_0}(\mathbf{y})} \underset{H_0}{\overset{H_1}{\gtrless}} \omega^2, \tag{3}$$

leading to the following test:

$$\Lambda_{\text{NMF-GLRT}} = \max_{\theta} \left|\mathbf{s}^H(\theta)\,\mathbf{u}\right|^2 \underset{\mathcal{H}_0}{\overset{\mathcal{H}_1}{\gtrless}} \omega^2, \tag{4}$$

with $\mathbf{s}(\theta) = \dfrac{\mathbf{R}^{-1/2}\,\mathbf{a}(\theta)}{\left\|\mathbf{R}^{-1/2}\,\mathbf{a}(\theta)\right\|}$ and $\mathbf{u} = \dfrac{\mathbf{R}^{-1/2}\,\mathbf{y}}{\left\|\mathbf{R}^{-1/2}\,\mathbf{y}\right\|}$.

Due to the presence of the maximum over θ, the statistic of this NMF-GLRT under $\mathcal{H}_0$ is complicated to derive. In [7], following a geometric approach [10], the authors have derived the expression of $P_{\text{fa}} = \mathbb{P}(\Lambda_{\text{NMF-GLRT}} \geq \omega^2 | \mathcal{H}_0)$ as a function of ω. This approach allows to understand the role of $\mathbf{R}$ more deeply.

Notice that testing only one single value of θ, leads to the well-known Normalized Matched Filter (NMF):

$$\Lambda_{\text{NMF}}(\theta) = \left|\mathbf{s}^H(\theta)\,\mathbf{u}\right|^2, \tag{5}$$

whose P_{fa}-threshold relationship is given by:

$$P_{\text{fa-NMF}} = (1-\omega^2)^{N-1}. \tag{6}$$

The NMF (5) has a constant false alarm rate, in the sense that the P_{fa}-threshold relationship is independent of $\mathbf{R}$ and of the testing point θ. This property is not at all verified by the NMF-GLRT. The P_{fa}-threshold relationship of the NMF-GLRT has been shown to depend on $\mathbf{R}$ in [7]. Omitting the edge effect term which is irrelevant when $\Theta = [0, 1[$, it may be shown that this relation can be written as:

$$P_{\text{fa}} \approx \frac{\Gamma(N)\,\omega(1-\omega^2)^{(2N-3)/2}}{\pi^{1/2}\,\Gamma\left(\dfrac{2N-1}{2}\right)} \int_{\Theta} v(\theta)\,d\theta, \tag{7}$$

where $v(\theta)$:

$$\begin{aligned} v(\theta) &= \left[\left\|\mathbf{s}'(\theta)\right\|^2 + \left(\mathbf{s}^H(\theta)\mathbf{s}'(\theta)\right)^2\right]^{1/2}, \\ &= \left[\left\|\mathbf{s}'(\theta)\right\|^2 - \left|\mathbf{s}^H(\theta)\mathbf{s}'(\theta)\right|^2\right]^{1/2}, \end{aligned} \tag{8}$$

due to the fact that $\mathbf{s}^H(\theta)\mathbf{s}(\theta) = 1$ implying that $\left(\mathbf{s}^H(\theta)\mathbf{s}(\theta)\right)' = 0$ and so $\text{Re}\left(\mathbf{s}^H(\theta)\mathbf{s}'(\theta)\right) = 0$. Equation (7) is a rewriting of [7], equation (15), considering directly the complex vector $\mathbf{s}(\theta)$ instead of dividing it into its real and imaginary parts.

In (7), the contribution $v(\theta)d\theta$ to the P_{fa} is proportional to the probability of false alarm in $[\theta, \theta + d\theta]$. When $\mathbf{R} = \mathbf{I}$, it is easy to check that $v(\theta)$ is constant, so that the false alarms are regularly distributed over $[0, 1[$. However, when $\mathbf{R} \neq \mathbf{I}$, $v(\theta)$ is no more constant and the density of false alarms is no more uniform over $[0, 1[$. In this sense, the action of $\mathbf{R}$ can thus be understood as a distortion of the manifold $\mathbf{s}(\Theta) \overset{\Delta}{=} \{\mathbf{s}(\theta), \theta \in \Theta\}$. Hence, the false alarm probability depends on $\mathbf{R}$.

Next, in order to implement the NMF-GLRT, we need to find the maximum of $\Lambda_{\text{NMF}}(.)$ over Θ. The general procedure to do so is the following one:

1) Define a grid of test points $\{\theta_i\}$.
2) Estimate the target location between test points, providing estimators $\left\{\hat{\theta}_i\right\}$.
3) Compute the $\Lambda_{\text{NMF}}(.)$ test on $\left\{\hat{\theta}_i\right\}$ and get the maximum of it.

In the next section, we propose a new way to define the grid taking into account the covariance matrix $\mathbf{R}$, and we see in Section IV how the estimates $\hat{\theta}_i$ are obtained.

III. A NEW GRID CONSTRUCTION TAKING THE COVARIANCE MATRIX INTO ACCOUNT

To compute the NMF-GLRT, equivalent to the maximum of the NMF over a continuous parameter space, the NMF has to be evaluated for discrete values of θ on a grid on Θ. This grid is usually regular over Θ. However, testing regular values of θ is not equivalent to testing points regularly spaced on the manifold $\mathbf{s}(\Theta)$, when $\mathbf{R} \neq \mathbf{I}$.

A. The distortion of the manifold

The distortion of the manifold depends on the noise covariance matrix $\mathbf{R}$ and has an impact on the shape of the main lobe corresponding to the true parameter θ_0 of the target. This can be evaluated mathematically using the ambiguity function $A_{\theta_0}(\theta)$, defined as the NMF test response at θ for a target characterized by parameter θ_0:

$$\begin{aligned} A_{\theta_0}(\theta) &= \left|\mathbf{s}^H(\theta)\,\mathbf{s}(\theta_0)\right|^2, \\ &= \text{Tr}(\mathbf{S}(\theta)\,\mathbf{S}(\theta_0)), \end{aligned} \tag{9}$$

where $\mathbf{S}(\theta) = \mathbf{s}(\theta)\,\mathbf{s}^H(\theta)$. So the shape of the main lobe is locally linked to the second-order derivative $A''_{\theta_0}(\theta_0)$.

As an example, Figure 1 shows a Power Spectral Density of the noise (directly connected to the covariance matrix $\mathbf{R}$ through Wiener Kintchin's Theorem). With such a noise, we get different lobe shapes for different values of θ_0 as described on this figure.

The most common case in radar detection is to face a white noise, meaning that $\mathbf{R} = \mathbf{I}$. In this case, a regular

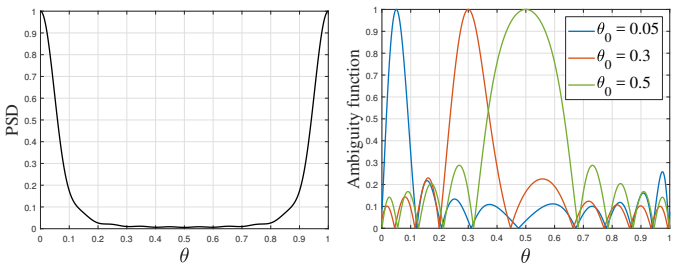

Figure 1. Power Spectral Density (PSD) and its corresponding lobe shapes.

grid on Θ: $(\theta_1, \theta_2, \ldots, \theta_M)$ corresponds to vectors on $\mathbf{s}(\Theta)$: $(\mathbf{s}(\theta_1), \ldots, \mathbf{s}(\theta_M))$ (usually, one chooses $M = N$, so that the grid step is equal to the conventional Doppler resolution). Please notice that in this case, the vectors $\{\mathbf{s}(\theta_i)\}$ are regularly spaced on the manifold described by $\mathbf{s}(\Theta)$.

To the best of our knowledge, even in colored noise when $\mathbf{R} \neq \mathbf{I}$, the procedure commonly used in radar is still to compute the NMF over a regular grid on Θ. In that case, we encounter distortion because $v(\theta)$ is no longer constant with respect to the usual parametrization of Θ.

As a consequence, although the grid $(\theta_1, \theta_2, \ldots, \theta_M)$ is regularly spaced over Θ, the test vectors $\{\mathbf{s}(\theta_i)\}$ are not regularly spaced on the manifold anymore. A solution we propose to circumvent this issue is to define a new grid on the parameter space Θ, which has the property to correspond to points regularly spaced on the manifold.

B. A new irregular grid

Let us define the function $\ell(.)$ as follows:

$$\ell : \theta \in \Theta \rightarrow x = \int_0^{\theta} v(u)\, du\,. \tag{10}$$

ℓ takes values in the interval $\mathcal{L} = [0, L_{\text{tot}}]$, where

$$L_{\text{tot}} = \ell(1) = \int_0^{1} v(u)\, du\ . \tag{11}$$

Once we have computed L_{tot}, we can slice it into M portions of the same size such that $(\ell(\theta_{i+1}) - \ell(\theta_i)) = \dfrac{L_{\text{tot}}}{M}$.

The proposed procedure provides a set of values $\{\theta_i\}$ that are not necessarily regularly spaced on Θ, but their corresponding vectors $\{\mathbf{s}(\theta_i)\}$ are regularly spaced on $\mathbf{s}(\Theta)$. This allows us to properly manage the distortion of the manifold.

C. Impact on the P_{fa} and on the lobe curvature

Concerning the P_{fa}, by construction and due to (7), on each interval $[\theta_i, \theta_{i+1}]$, the P_{fa} is constant.

We will now focus on the lobe shape and prove that the proposed reparametrization provides main lobes that are locally identical. This is the object of the following Lemma.

Lemma 1. *The second-order derivative of $A_{\theta_0} \circ \ell^{-1}$ in $x = x_0$, such that $\ell^{-1}(x_0) = \theta_0$, is independent of θ_0.*

Proof. Since $\mathbf{s}(\theta)$ is normalized, we have for any θ:

$$\text{Tr}(\mathbf{S}(\theta)\, \mathbf{S}(\theta)) = 1\,. \tag{12}$$

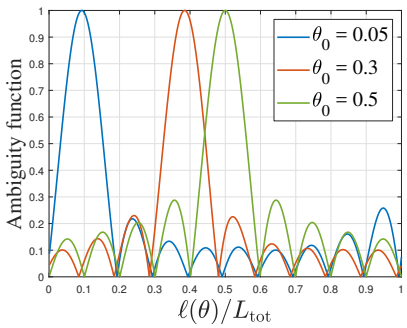

Figure 2. Reparameterized lobe shapes.

By deriving twice (12), we get:

$$\begin{cases} \text{Tr}(\mathbf{S}'(\theta)\, \mathbf{S}(\theta)) = 0\,, \\ \text{Tr}\left(\mathbf{S}''(\theta)\, \mathbf{S}(\theta)\right)) + \text{Tr}\left(\mathbf{S}'(\theta)\, \mathbf{S}'(\theta)\right) = 0\ . \end{cases} \tag{13}$$

Hence, since $A''_{\theta_0}(\theta) = \text{Tr}\left(\mathbf{S}''(\theta)\, \mathbf{S}(\theta_0)\right)$, we can deduce that:

$$A''_{\theta_0}(\theta_0) = -\text{Tr}(\mathbf{S}'(\theta_0)\, \mathbf{S}'(\theta_0))\,. \tag{14}$$

Since we have:

$$\mathbf{S}'(\theta) = \mathbf{s}'(\theta)\, \mathbf{s}^H(\theta) + \mathbf{s}(\theta)\, \mathbf{s}'^H(\theta)\,, \tag{15}$$

we can use the linearity of the trace and its invariance with respect to circular permutations, as well as the fact that $\mathbf{s}^H(\theta)\mathbf{s}'(\theta)$ is pure imaginary (see the end of Section II) so that $\left(\mathbf{s}^H(\theta)\mathbf{s}'(\theta)\right)^2$ is real, to get:

$$\text{Tr}(\mathbf{S}'(\theta)\, \mathbf{S}'(\theta)) = 2\left(\mathbf{s}'^H(\theta)\, \mathbf{s}'(\theta) + (\mathbf{s}^H(\theta)\, \mathbf{s}'(\theta))^2\right)\ . \tag{16}$$

Now, we just need to use the chain rule and the fact that $A'_{\theta_0}(\theta_0) = 0$ to see that:

$$\begin{aligned} A''_{\theta_0}\left(\ell^{-1}(x_0)\right) &= -2\left[\left(\ell^{-1}\right)'(x_0)\right]^2 \left[\|\mathbf{s}'(\theta_0)\|^2\right. \\ &\quad \left. +(\mathbf{s}^H(\theta_0)\, \mathbf{s}'(\theta_0))^2\right] \qquad (17) \\ &= -2\left[\left(\ell^{-1}\right)'(x_0)\right]^2 v^2(\theta_0)\,. \qquad (18) \end{aligned}$$

Note that by definition of the function ℓ^{-1}, we have

$$\left(\ell^{-1}\right)'(x_0) = \frac{1}{v \circ \ell^{-1}(x_0)} = \frac{1}{v(\theta_0)}\,, \tag{19}$$

where $v(\theta_0)$ is given by (8). We finally get:

$$A''_{\theta_0}\left(\ell^{-1}(x_0)\right) = -2\,. \tag{20}$$

□

Using this Lemma, we can conclude that all the main lobes have locally the same shape in the reparameterized space. Thus, the criterion initially based on the P_{fa} has interesting properties for the detection probability.

In the next section, we analyze different approaches to evaluate the NMF-GLRT.

IV. A CONTINUOUS APPROACH USING JOINT ESTIMATION-DETECTION TECHNIQUES

The final objective is to perform the NMF-GLRT. The general procedure to do so (without using to much computational power and time) is described at the end of Section II and different approaches are now presented.

A. Standard monopulse processing

A popular approach in radar context is the monopulse technique [5]. It is a cost efficient approximation of the maximum likelihood of the target parameter. The principle is the following one:

1) The grid is initialized with regularly spaced values $\{\theta_1, \ldots, \theta_N\}$ with a step $\delta_\theta = \dfrac{1}{N}$ corresponding to the Doppler resolution.

2) The parameter estimations $\{\hat{\theta}_i\}$ between two grid points are performed based on the monopulse principle:

$$\hat{\theta}_i = \frac{\theta_i + \theta_{i+1}}{2} + \frac{\delta_\theta}{2} \frac{\Lambda_{\text{NMF}}\left(\theta_{i+1}\right)^{\frac{1}{2}} - \Lambda_{\text{NMF}}\left(\theta_i\right)^{\frac{1}{2}}}{\Lambda_{\text{NMF}}\left(\theta_{i+1}\right)^{\frac{1}{2}} + \Lambda_{\text{NMF}}\left(\theta_i\right)^{\frac{1}{2}}} . \quad (21)$$

3) Since we need to perform the NMF test on $\{\theta_i\}$ in order to estimate $\{\hat{\theta}_i\}$, the approximation of the NMF-GLRT corresponding to this method corresponds to:

$$\hat{\Lambda}_{\text{NMF-GLRT}} = \max_{\theta \in \{\theta_i\} \cup \left\{\hat{\theta}_i\right\}} \Lambda_{\text{NMF}}\left(\theta\right) . \quad (22)$$

As shown in the numerical part, when the covariance matrix $\mathbf{R}$ is different from the identity matrix $\mathbf{I}$, the estimations $\hat{\theta}_i$ are not really relevant since the distortion of the manifold is not considered at all. Thus, even when the SNR tends to infinity, some targets are not detected.

B. A first way to face distortion: estimate before distortion

To circumvent the estimation issue in the case $\mathbf{R} \neq \mathbf{I}$, the method proposed in [8] is the following one:

1) Same regular grid as in IV-A.

2) The parameter estimations $\left\{\hat{\theta}_i\right\}$ between two grid points are performed based on the monopulse principle but on the Discrete Fourier Transform (DFT) of the signal $\mathbf{y}$ and a well chosen function g:

$$\hat{\theta}_i = \frac{\theta_i + \theta_{i+1}}{2} + g^{-1}\left(\frac{\left|\mathbf{a}^H(\theta_{i+1})\,\mathbf{y}\right|^2 - \left|\mathbf{a}^H(\theta_i)\,\mathbf{y}\right|^2}{\left|\mathbf{a}^H(\theta_{i+1})\,\mathbf{y}\right|^2 + \left|\mathbf{a}^H(\theta_i)\,\mathbf{y}\right|^2} \right) , \quad (23)$$

With g defined in [8], equation (9).

3) Finally, the approximation of the NMF-GLRT corresponding to this method corresponds to:

$$\hat{\Lambda}_{\text{NMF-GLRT}} = \max_{\theta \in \left\{\hat{\theta}_i\right\}} \Lambda_{\text{NMF}}\left(\theta\right) . \quad (24)$$

This is a better way to estimate $\hat{\theta}_i$ because if we do not introduce $\mathbf{R}$ in the first stage and use the DFT, the lobe shape has not yet been modified and hence the monopulse estimation technique is more relevant at high SNR.

However, since we do not take into account the impact of $\mathbf{R}$ in the estimation part, there are still some losses especially when the SNR is moderate.

C. Monopulse reparametrized (proposed)

In this article, we propose to address the distortion issue by reparametrizing our manifold. Instead of working directly in the space Θ, we work in the space $\mathcal{L} = \ell(\Theta)$ and use the function ℓ^{-1} when it is necessary to go back to Θ.

1) The grid is initialized with regularly spaced values $\{x_i\}$ on $\mathcal{L}$, corresponding to irregularly spaced values $\{\theta_1, \ldots, \theta_N\} = \{\ell^{-1}(x_1), \ldots, \ell^{-1}(x_N)\}$, as described in III-B. The step between two successive points x_i on $\mathcal{L}$ is $\delta_x = \dfrac{L_{\text{tot}}}{N}$.

2) The estimations $\{\hat{x}_i\}$, between two grid points are performed based on the monopulse principle but on the reparameterized space with $x = \ell(\theta)$:

$$\hat{x}_i = \frac{x_i + x_{i+1}}{2} + \frac{\delta_x}{2} \frac{\Lambda_{\text{NMF}}\left(\ell^{-1}(x_{i+1})\right)^{\frac{1}{2}} - \Lambda_{\text{NMF}}\left(\ell^{-1}(x_i)\right)^{\frac{1}{2}}}{\Lambda_{\text{NMF}}\left(\ell^{-1}(x_{i+1})\right)^{\frac{1}{2}} + \Lambda_{\text{NMF}}\left(\ell^{-1}(x_i)\right)^{\frac{1}{2}}} . \quad (25)$$

3) Since we need to perform the NMF test on $\{\ell^{-1}(x_i)\}$ in order to estimate $\{\hat{x}_i\}$, the approximation of the NMF-GLRT corresponding to this method corresponds to:

$$\hat{\Lambda}_{\text{NMF-GLRT}} = \max_{x \in \{x_i\} \cup \{\hat{x}_i\}} \Lambda_{\text{NMF}}\left(\ell^{-1}(x)\right) . \quad (26)$$

Please note that the computational task of performing ℓ^{-1} is negligible since ℓ can be tabuled (and so ℓ^{-1} too).

V. NUMERICAL EXPERIMENTS

In this part, we compare the performance of the different methods. We plot, for two different covariance matrices, the detection probability of each method as a function of the target parameter θ and as a function of the SNR, defined as $\text{SNR}(\alpha, \theta) = \dfrac{|\alpha|^2}{\left\|\mathbf{R}^{-1/2}\,\mathbf{a}(\theta)\right\|^2}$. The first covariance $\mathbf{R}_1$ corresponds to the noise Power Spectral Density plotted in Figure 1, while the second one $\mathbf{R}_2$ corresponds to the matrix $\mathbf{R}(0.95)$ using the classical Toeplitz model of noise clutter:

$$\mathbf{R}(\rho) = \mathcal{T}([1, \rho, \ldots, \rho^{N-1}]) , \quad (27)$$

where $\mathcal{T}(.)$ is the Toeplitz operator.

In all the experiments we performed, the proposed method was shown to maintain constant performance, regardless of the target parameter and the noise covariance matrix, and performs better than the others in any context as it can be noticed in Figures 3 and 4. Its computational cost is twice that of the on-grid algorithm (since we perform twice more NMF tests) and is equivalent to the state-of-the-art techniques used in the numerical experiments.

Moreover, the P_{fa} (computed using Monte Carlo experiments) corresponding to the proposed strategy, in red in Figure 5, is the closest to the theoretical false alarm probability provided in Eq.(7). This is another indicator that we are performing the most accurate approximation of the NMF-GLRT at a very low cost.

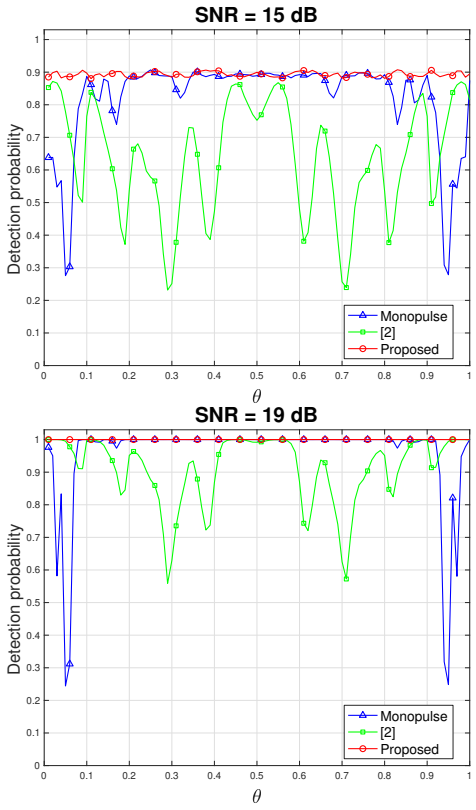

Figure 3. Detection performances comparison, with $\mathbf{R} = \mathbf{R}_1$, using the same threshold ω^2 for all methods such that the theoretical P_{fa} is 10^{-3} in (7).

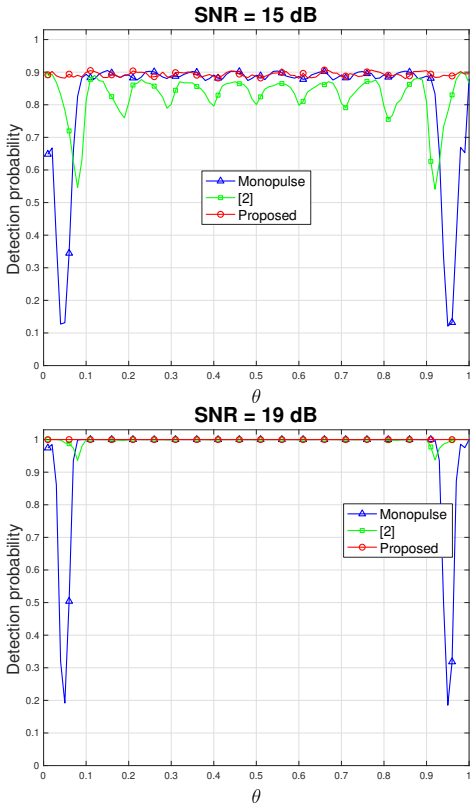

Figure 4. Detection performances comparison, with $\mathbf{R} = \mathbf{R}_2$, using the same threshold ω^2 for all methods such that the theoretical P_{fa} is 10^{-3} in (7).

VI. Conclusion

In this paper, we proposed a solution to the off-grid issue faced by the NMF test. In particular, we introduced an irregular test grid strategy and a joint estimation-detection method. Our main contribution was to consider the deformation of the manifold induced by the covariance matrix to provide an efficient detection method relying on a reparametrization. The numerical experiments show that we perform the best approximation of the NMF-GLRT performances at a very low cost. Finally, this procedure can be directly extended to the off-grid Matched Filter using the exact same reparametrization.

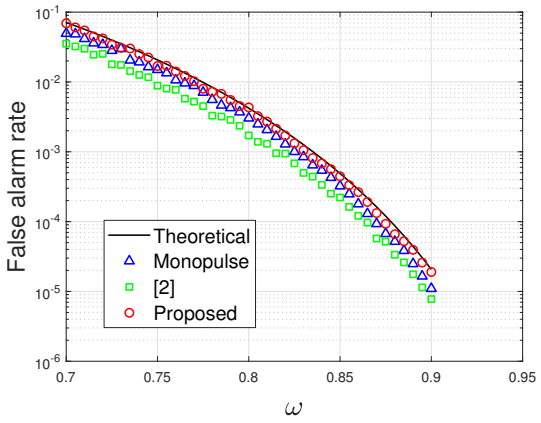

Figure 5. P_{fa}-threshold relationship comparison with $\mathbf{R} = \mathbf{R}_1$

References

[1] Kay, S. M. (1993). Fundamentals of statistical signal processing: estimation theory. Prentice-Hall, Inc..

[2] Scharf, L. L., Demeure, C. (1991). Statistical signal processing: detection, estimation, and time series analysis. Addison-Wesley Publishing Company.

[3] Conte, E., Lops, M., Ricci, G. (1996). Adaptive Matched Filter detection in spherically invariant noise. IEEE Signal Processing Letters, 3(8), 248-250.

[4] Kraut, S., Scharf, L. L., McWhorter, L. T. (2001). Adaptive subspace detectors. IEEE Transactions on Signal Processing, 49(1), 1-16.

[5] Sherman, S. M., Barton, D. K. (2011). Monopulse principles and techniques. Artech House.

[6] Rabaste, O., Bosse, J., Ovarlez, J.-P. (2016, August). Off-grid target detection with Normalized Matched subspace filter. In 2016 24th European Signal Processing Conference (EUSIPCO) (pp. 1926-1930).

[7] Develter, P., Bosse, J., Rabaste, O., Forster, P., Ovarlez, J.-P. (2024). On the False Alarm Probability of the Normalized Matched Filter for off-grid targets: A geometrical approach and its validity conditions. IEEE Transactions on Signal Processing, 72, pp.982-996.

[8] Develter, P., Bosse, J., Rabaste, O., Forster, P., Ovarlez, J.-P. (2021, July). Off-grid radar target detection with the Normalized Matched Filter: A monopulse-based detection scheme. In 2021 IEEE Statistical Signal Processing Workshop (SSP) (pp. 226-230). IEEE.

[9] Ollila, E., Tyler, D. E., Koivunen, V., Poor, H. V. (2012). Complex elliptically symmetric distributions: Survey, new results and applications. IEEE Transactions on Signal Processing, 60(11), 5597-5625.

[10] Weyl, H. (1939). On the volume of tubes. American Journal of Mathematics, 61(2), 461-472.